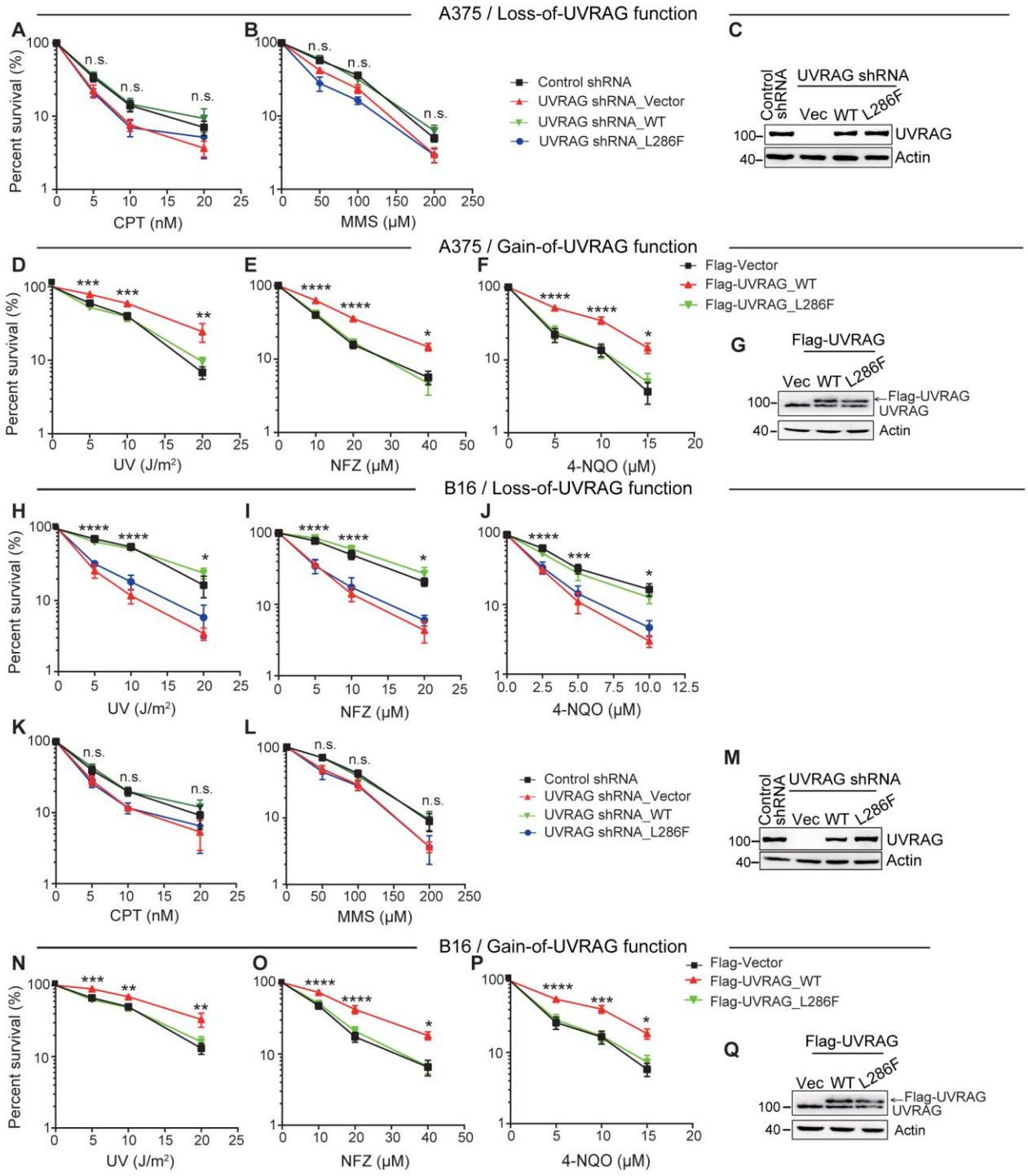


Figure S1

**Figure S1 Effect of UVRAG on Sensitivity of Melanoma Cells to UV-induced DNA Damage.**

Related to Figure 1.

(A-C) Colony survival assays of A375 cells expressing control shRNA or UVRAG-specific shRNA transduced with empty retroviral vector (UVRAG shRNA_Vector), with retroviral vector expressing WT human UVRAG (UVRAG shRNA_WT), or with retroviral vector expressing UVRAG L286F point-mutant (UVRAG shRNA_L286F). Cells were exposed to the indicated doses of the DNA topoisomerase inhibitor, Camptothecin (CPT; A) and the DNA replication inhibitor, methylmethanesulphonate (MMS; B), followed by colony survival assay. UVRAG expression was assessed by immunoblotting and compared to actin levels (C). Data are mean ± SD from three independent experiments. n.s., not statistically significant.

(D-G) Increased UV-resistance of A375 cells upon ectopic expression of UVRAG. A375 cells stably expressing Flag-tagged empty vector (Vector), WT UVRAG (UVRAG_WT), or UVRAG_L286F point-mutant were subjected to the indicated doses of UV-C irradiation (D) or UV-mimetic agents including NFZ (E) and 4-NQO (F), followed by colony survival assay. UVRAG expression was assessed by immunoblotting (G). Data are mean ± SD from three independent experiments. * $p < 0.05$; ** $p < 0.01$; *** $p < 0.001$; **** $p < 0.0001$ (UVRAG_WT vs. Vector).

(H-M) Sensitivity of mouse melanoma B16 cells with shRNA-mediated knockdown of *UVRAG* complemented with an empty vector (UVRAG shRNA_Vector), or with shRNA-resistant WT UVRAG (UVRAG shRNA_WT), or UVRAG L286F point-mutant (UVRAG shRNA_L286F), to UV-C irradiation (H), UV-mimetic reagents, NFZ (I), and 4-NQO (J), or to CPT (K), and MMS (L), as determined by colony-forming ability. The expression of UVRAG and actin was assessed by immunoblotting (M). Data are mean ± SD from three independent experiments. n.s., not statistically significant. *$p < 0.05$; ***$p < 0.001$; ****$p < 0.0001$ (UVRAG_shRNA_Vector vs. Control shRNA).

(N-Q) Sensitivity of mouse melanoma B16 cells stably expressing WT UVRAG (UVRAG_WT), or UVRAG L286F (UVRAG_L286F) point-mutant to UV-C irradiation (N) and UV-mimetic reagents, NFZ (O) and 4-NQO (P), as determined by colony-forming ability. The expression of Flag-UVRAG and actin was assessed by immunoblotting (Q). Data are mean ± SD from three independent experiments. *$p < 0.05$; **$p < 0.01$; ***$p < 0.001$; ****$p < 0.0001$ (UVRAG_WT vs. Vector).

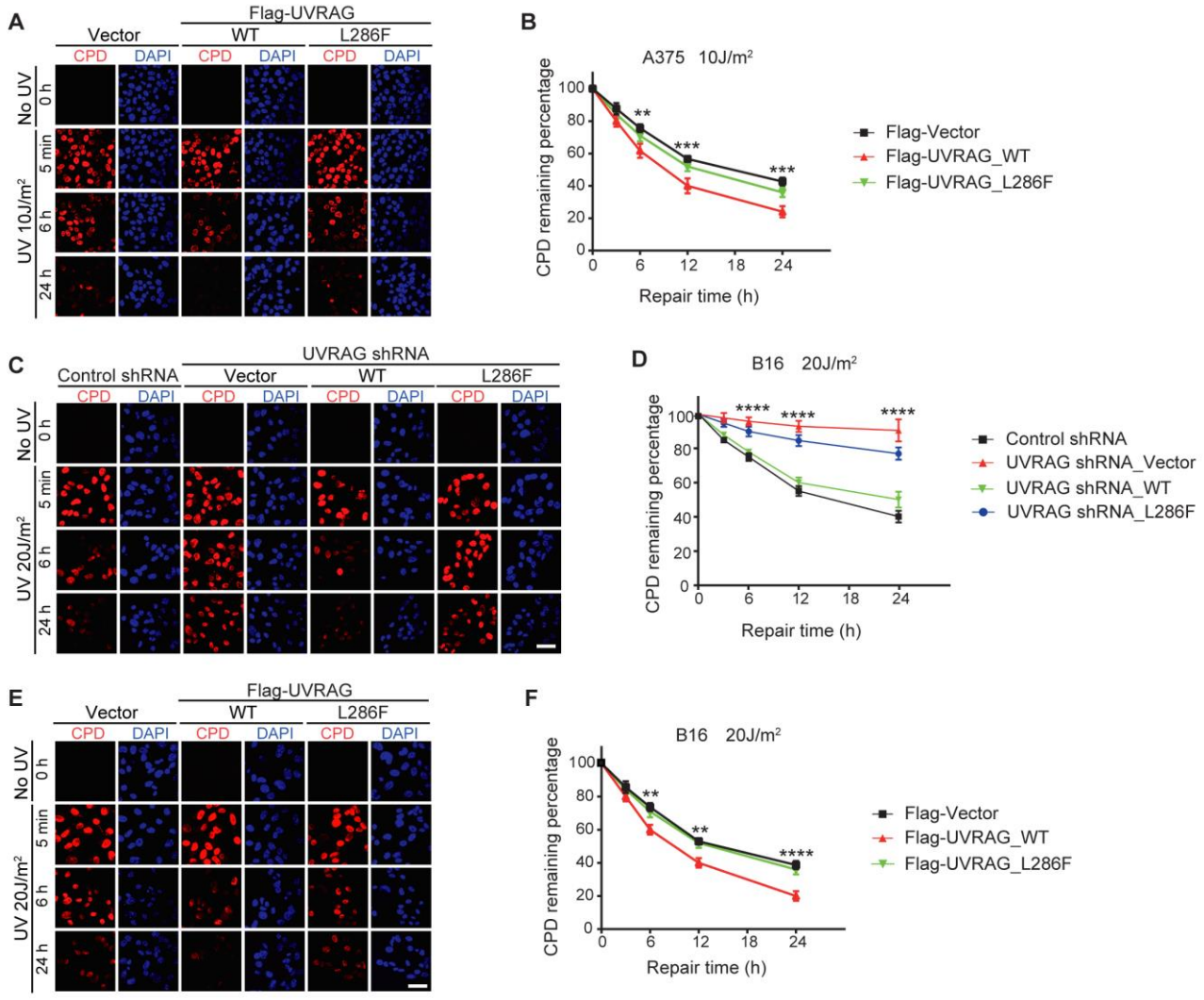


Figure S2

**Figure S2 UVRAG Is Required for UV-induced DNA Damage Repair.** Related to Figure 1

(A and B) Increased rate of CPD repair upon gain-of-UVRAG function in human melanoma cells. A375 cells stably expressing an empty vector, WT UVRAG, or with UVRAG L286F point-mutant were treated with UV-C and allowed to recover for a period of time as indicated. Quantification of the percentage of remaining CPD per cell relative to that of 0 hr after UV-C in each sample is plotted (B). Representative CPD images are shown in (A). Scale bar, 20 μm. $^{**}p < 0.01$; $^{***}p < 0.001$ (UVRAG_WT vs. Vector).

(C and D) Delay of CPD repair with UVRAG deficiency in mouse melanoma cells. B16 cells stably expressing control shRNA, or UVRAG-specific shRNA complemented with an empty vector, WT UVRAG, or with the UVRAG L286F point-mutant, were treated with UV and allowed to recover for a period of time as indicated. Representative CPD images are shown in (C) and quantification of the percentage of remaining CPD per cell relative to that of 0 hr after UV-C in each sample is plotted (D). Scale bar, 20 μm. ****$p < 0.0001$ (UVRAG shRNA_Vector vs. Control shRNA).

(E and F) Increased rate of CPD repair upon gain-of-UVRAG function in mouse melanoma cells. B16 cells stably expressing an empty vector, WT UVRAG, or with the UVRAG L286F point-mutant were treated with UV and allowed to recover for a period of time as indicated. Representative CPD images are shown in (E) and quantification of the percentage of remaining CPD per cell relative to that of 0 hr after UV-C in each sample is plotted (F). Scale bar, 20 μm. **$p < 0.01$; ****$p < 0.0001$ (UVRAG_WT vs. Vector).

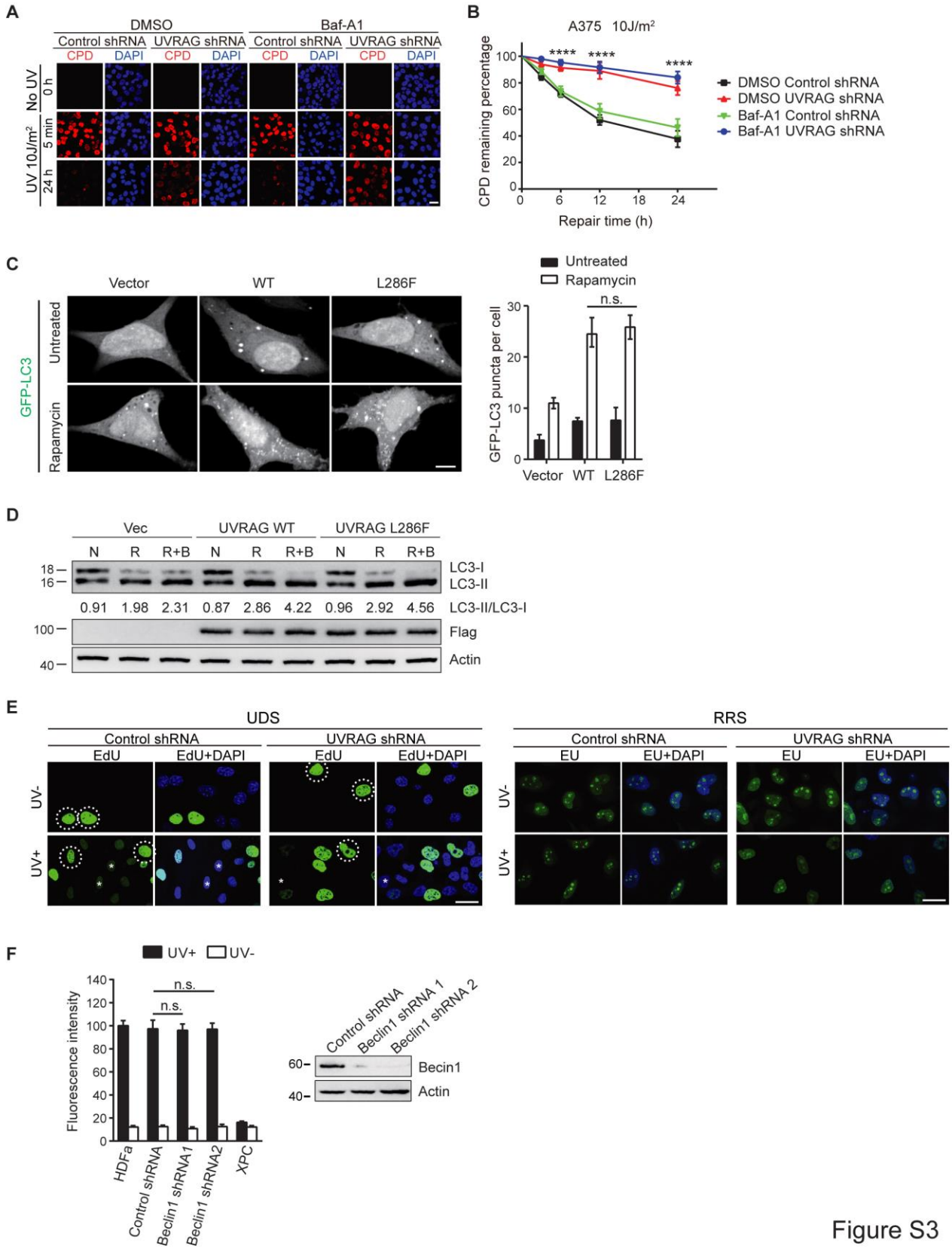


**Figure S3 Autophagy-independent Effect of UVRAG in NER.** Related to Figure 1

(A and B) UVRAG knockdown delayed the rate of UV-induced CPD repair in Bafilomycin A1 (Baf-A1)-treated A375 cells. The A375 cells stably expressing control shRNA or UVRAG-specific shRNA were treated with DMSO or Baf-A1 (100 nM) for 1 hr and then subjected to UV-C irradiation and allowed to recover for a period of time as indicated. Representative images of confocal microscopy for CPD staining (red) are shown in (A). The percentage of remaining CPD per cell relative to that of 0 hr after UV-C in each sample is plotted (B). Scale bar, 20 μm. Data are mean ± SD from three independent experiments. ****$p < 0.0001$ (Baf-A1 UVRAG shRNA vs. Baf-A1 Control shRNA).

(C) UVRAG L286F retains the activity of WT in autophagy regulation. HeLa cells stably expressing vector, WT, and L286F mutant were transfected with GFP-LC3 and treated with rapamycin. GFP-LC3 puncta per cell were quantified (right) as shown in representative images (left). Scale bar, 10 μm. n.s., not significant.

(D) Western blot analysis and densitometric quantification (underneath the blot) of the LC3-II/LC3-I ratios in HeLa cells treated with rapamycin in the presence or absence of Bafilomycin A1. N, normal condition; R, rapamycin; R+B, rapamycin+Bafilomycin A1.

(E) Typical UDS and RRS images are shown. A375 cells in Figure 1H stably expressing control shRNA or UVRAG shRNA were UV-irradiated (+UV) or mock-treated (-UV), followed by the EdU-incorporation (for UDS) or EU incorporation (for RRS). Asterisks highlight non-S phase cells used for the fluorescence calculation in UDS; dashed circles indicate the S-phase cells excluded from the UDS analysis. Scale bar, 20 μm.

(F) Knockdown of Beclin1 does not affect the UDS activity after UV irradiation. HeLa cells expressing control shRNA or two independent Beclin1-specific shRNA were UV-C-irradiated and subjected to UDS assay. UDS activity in XPC-deficient cells served as the control. Filled bars, UV-irradiated; open bars, no UV. Note the close-to-normal UDS in the Beclin1-knockdown cells. Beclin1 expression is detected by immunoblotting (right). Data shown represent mean ± SD from three independent experiments. n.s., not significant.

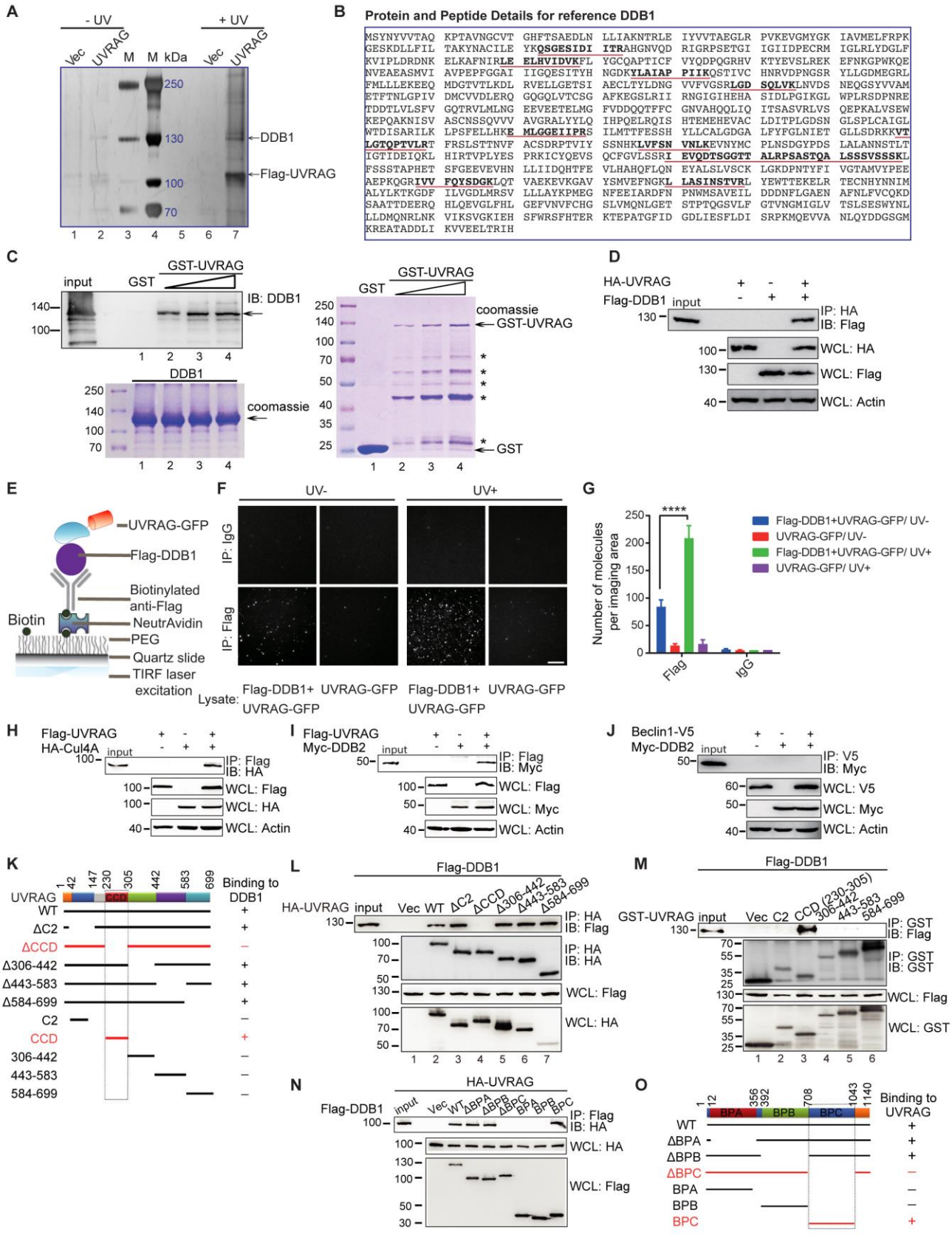
A
- UV
+ UV
Vec
UVRAG
M
M kDa
Vec
UVRAG
250
130
100
70
DDB1
Flag-UVRAG
1 2 3 4 5 6 7
B
Protein and Peptide Details for reference DDB1
MSYNYVVTAQ KPTAVNGCVT GHFTSAEDLN LLIAKNTRLE IYVVTAEGLR PVKEVGMYGK IAVMELFRPK
GESKDLLFIL TAKYNACILE YKQSGESIDI ITRAHGNVQD RIGRPSETGI IGIIDPECRM IGLRLYDGLF
KVIPLDRDNK ELKAFNIRLE ELHVIDVKFL YGCQAPTICF VYQDPQGRHV KTYEVSLREK EFNKGPWKQE
NVEAEASMVI AVPEPFGGAI IIGQESITYH NGDKYLAIAP PIIKQSTIVC HNRVDPNGSR YLLGDMEGRL
FMLLLEKEEQ MDGTVTLKDL RVELLGETSI AECLTYLDNG VVFVGSRLGD SQLVKLNVDS NEQGSYVVAM
ETFTNLGPIV DMCVVDLERQ GQGQLVTCSG AFKEGSLRII RNGIGIHEHA SIDLPGIKGL WPLRSDPNRE
TDDTLVLSFV GQTRVLMLNG EEVEETELMG FVDDQQTFFC GNVAHQQLIQ ITSASVRLVS QEPKALVSEW
KEPQAKNISV ASCNSSQVVV AVGRALYYLQ IHPQELRQIS HTEMEHEVAC LDITPLGDSN GLSPLCAIGL
WTDISARILK LPSFELLHKE MLGGEIIPRS ILMTTFESSH YLLCALGDGA LFYFGLNIET GLLSDRKKVT
LGTQPTVLRT FRSLSTTNVF ACSDRPTVIY SSNHKLVFSN VNLKEVNYMC PLNSDGYPDS LALANNSTLT
IGTIDEIQKL HIRTVPLYES PRKICYQEVS QCFGVLSSRI EVQDTSGGTT ALRPSASTQA LSSSVSSSKL
FSSSTAPHET SFGEEVEVHN LLIIDQHTFE VLHAHQFLQN EYALSLVSCK LGKDPNTYFI VGTAMVYPEE
AEPKQGRIVV FQYSDGKLQT VAEKEVKGAV YSMVEFNGKL LASINSTVRL YEWTTEKELR TECNHYNNIM
ALYLKTKGDF ILVGDLMRSV LLLAYKPMEG NFEEIARDFN PNWMSAVEIL DDDNFLGAEN AFNLFVCQKD
SAATTDEERQ HLQEVGLFHL GEFVNVFCHG SLVMQNLGET STPTQGSVLF GTVNGMIGLV TSLSESWYNL
LLDMQNRLNK VIKSVGKIEH SFWRSFHTER KTEPATGFID GDLIESFLDI SRPKMQEVVA NLQYDDGSGM
KREATADDLI KVVEELTRIH
C
input
GST
GST-UVRAG
IB: DDB1
140
100
1 2 3 4
DDB1
250
140
100
70
coomassie
GST-UVRAG
GST
250
140
100
70
50
40
35
25
coomassie
GST-UVRAG
*
*
*
*
*
GST
1 2 3 4
D
HA-UVRAG
Flag-DDB1
input
130
IP: HA
IB: Flag
100
WCL: HA
130
WCL: Flag
40
WCL: Actin
E
UVRAG-GFP
Flag-DDB1
Biotinylated anti-Flag
NeutrAvidin
PEG
Quartz slide
TIRF laser excitation
Biotin
F
UV-
UV+
IP: IgG
IP: Flag
Lysate:
Flag-DDB1+ UVRAG-GFP
UVRAG-GFP
Flag-DDB1+ UVRAG-GFP
UVRAG-GFP
G
Number of molecules per imaging area
250
200
150
100
50
0
****
Flag-DDB1+UVRAG-GFP/ UV-
UVRAG-GFP/ UV-
Flag-DDB1+UVRAG-GFP/ UV+
UVRAG-GFP/ UV+
Flag
IgG
H
Flag-UVRAG
HA-Cul4A
input
100
IP: Flag
IB: HA
100
WCL: Flag
100
WCL: HA
40
WCL: Actin
I
Flag-UVRAG
Myc-DDB2
input
50
IP: Flag
IB: Myc
100
WCL: Flag
50
WCL: Myc
40
WCL: Actin
J
Beclin1-V5
Myc-DDB2
input
50
IP: V5
IB: Myc
60
WCL: V5
50
WCL: Myc
40
WCL: Actin
K
UVRAG
1 42 147 230 305 442 583 699
CCD
Binding to DDB1
WT +
ΔC2 +
ΔCCD –
Δ306-442 +
Δ443-583 +
Δ584-699 +
C2 –
CCD +
306-442 –
443-583 –
584-699 –
L
Flag-DDB1
HA-UVRAG
input
Vec
WT
ΔC2
ΔCCD
Δ306-442
Δ443-583
Δ584-699
130
IP: HA
IB: Flag
100
70
50
IP: HA
IB: HA
130
WCL: Flag
100
70
50
WCL: HA
1 2 3 4 5 6 7
M
Flag-DDB1
GST-UVRAG
input
Vec
C2
CCD (230-305)
306-442
443-583
584-699
130
IP: GST
IB: Flag
70
55
35
25
IP: GST
IB: GST
130
WCL: Flag
70
55
35
25
WCL: GST
1 2 3 4 5 6
N
HA-UVRAG
Flag-DDB1
input
Vec
WT
ΔBPA
ΔBPB
ΔBPC
BPA
BPB
BPC
100
IP: Flag
IB: HA
100
WCL: HA
130
100
WCL: Flag
50
30
O
1 12 356 392 708 1043 1140
BPA
BPB
BPC
Binding to UVRAG
WT +
ΔBPA +
ΔBPB +
ΔBPC –
BPA –
BPB –
BPC +

Figure S4

**Figure S4 UVRAG Forms A Complex with the CRL4$^{DDB2}$ E3 Ligase Complex.** Related to Figure 2

(A and B) Identification of UVRAG-interacting proteins upon UV irradiation. A375 cells stably expressing empty vector (lane 1 and 6) or Flag-UVRAG (lane 2 and 7) were collected before (- UV) and after UV treatment (+ UV) for immune-purification with Flag-conjugated agarose beads and the purified proteins were detected by silver staining (A). Proteins are identified based on mass spectrometry results combined with predicted molecular weights. The multiple peptides of DDB1 were identified in the immunocomplex of UVRAG by mass spectrometry (B).

(C) Purified UVRAG directly interacts with recombinant DDB1 *in vitro.* Increasing amount of purified GST only (control) or GST-UVRAG were mixed with DDB1 and subjected to GST-pulldown followed by IB for DDB1. Efficient DDB1-UVRAG interaction was detected in a dose-dependent manner (lane 2-4). Coomassie blue stainings show input of each purified proteins used for binding. Asterisks indicate degradation products of GST-UVRAG.

(D) UVRAG interacts with DDB1. 293T cells were co-transfected with HA-UVRAG and Flag-DDB1. At 48 hr post-transfection, WCL treated with nucleases were used for immunoprecipitation (IP) with anti-HA, followed by immunoblotting (IB) with anti-Flag.

(E) Schematic representation of SiMPull assay to examine the UVRAG-DDB1 interaction at single molecule level.

(F) UV irradiation increases the UVRAG-DDB1 complex formation. 293T cells co-expressing FLAG-DDB1 and UVRAG-GFP were UV irradiated and the cell lysates were subjected to SiMPull. Representative SiMPull images of GFP-fluorescence from anti-Flag (bottom panel) or control antibody (top panel) coated surface incubated with the indicated lysates are shown. Note the increased GFP-fluorescence spots after UV treatment. Scale bar, 5 μm.

(G) Average number of fluorescent molecules per imaging area was quantified for each sample. Error bars denote standard deviation (s.d.) (n = 5). ****, $p < 0.0001$.

(H) UVRAG interacts with Cul4A. 293T cells were co-transfected with Flag-UVRAG and HA-Cul4A. At 48 hr post-transfection, WCL were used for IP with anti-Flag followed by IB with anti-HA.

(I) UVRAG interacts with DDB2. 293T cells were co-transfected with Flag-UVRAG and Myc-DDB2. At 48 hr post-transfection, WCL were used for IP with anti-Flag followed by IB with anti-Myc.

(J) Beclin1 does not interact with DDB2. 293T cells were co-transfected with Beclin1-V5 and Myc-DDB2. At 48 hr post-transfection, WCL were used for IP with anti-V5 followed by IB with anti-Myc.

(K) Schematic representation of WT UVRAG and its deletion mutants and summary of their interactions with DDB1. Interaction was determined by coimmunoprecipitation of Flag-UVRAG with endogenous DDB1 from 293T cell lysates. Putative UVRAG protein domains predicted by the Ensembl database are highlighted. C2, lipid-binding domain; CCD, coiled-coil domain. +, strong binding; -, no binding.

(L) UVRAG interaction with DDB1 requires its coiled-coiled domain (CCD). 293T cells were transfected with Flag-DDB1 along with HA-UVRAG or its mutant derivatives. WCL were subjected to immunoprecipitation with an anti-HA antibody, followed by IB with anti-Flag or anti-HA. WCL were also used for IB with the indicated antibodies to show expression.

(M) UVRAG CCD interacts with DDB1. 293T cells were co-transfected with Flag-DDB1, together with GST-tagged vector or UVRAG mutants ($UVRAG^{C2}$, $UVRAG^{CCD}$, $UVRAG^{306\text{-}442}$, $UVRAG^{443\text{-}583}$, $UVRAG^{584\text{-}699}$). At 48 hr post-transfection, WCL were used for GST-pull down, followed by IB with anti-Flag or anti-GST.

(N) The BPC domain of DDB1 interacts with UVRAG. 293T cells were co-transfected with HA-UVRAG, together with Flag-tagged vector or DDB1 mutants ($DDB1^{\Delta BPA}$, $DDB1^{\Delta BPB}$, $DDB1^{\Delta BPC}$, $DDB1^{BPA}$, $DDB1^{BPB}$, $DDB1^{BPC}$). At 48 hr post-transfection, WCL were used for IP with anti-Flag followed by IB with anti-HA.

(O) Schematic representation of WT DDB1 and its deletion mutants, and summary of their interactions with UVRAG. Interaction was determined by coimmunoprecipitation of Flag-DDB1 with HA-UVRAG from 293T cell lysates. +, strong binding; -, no binding.

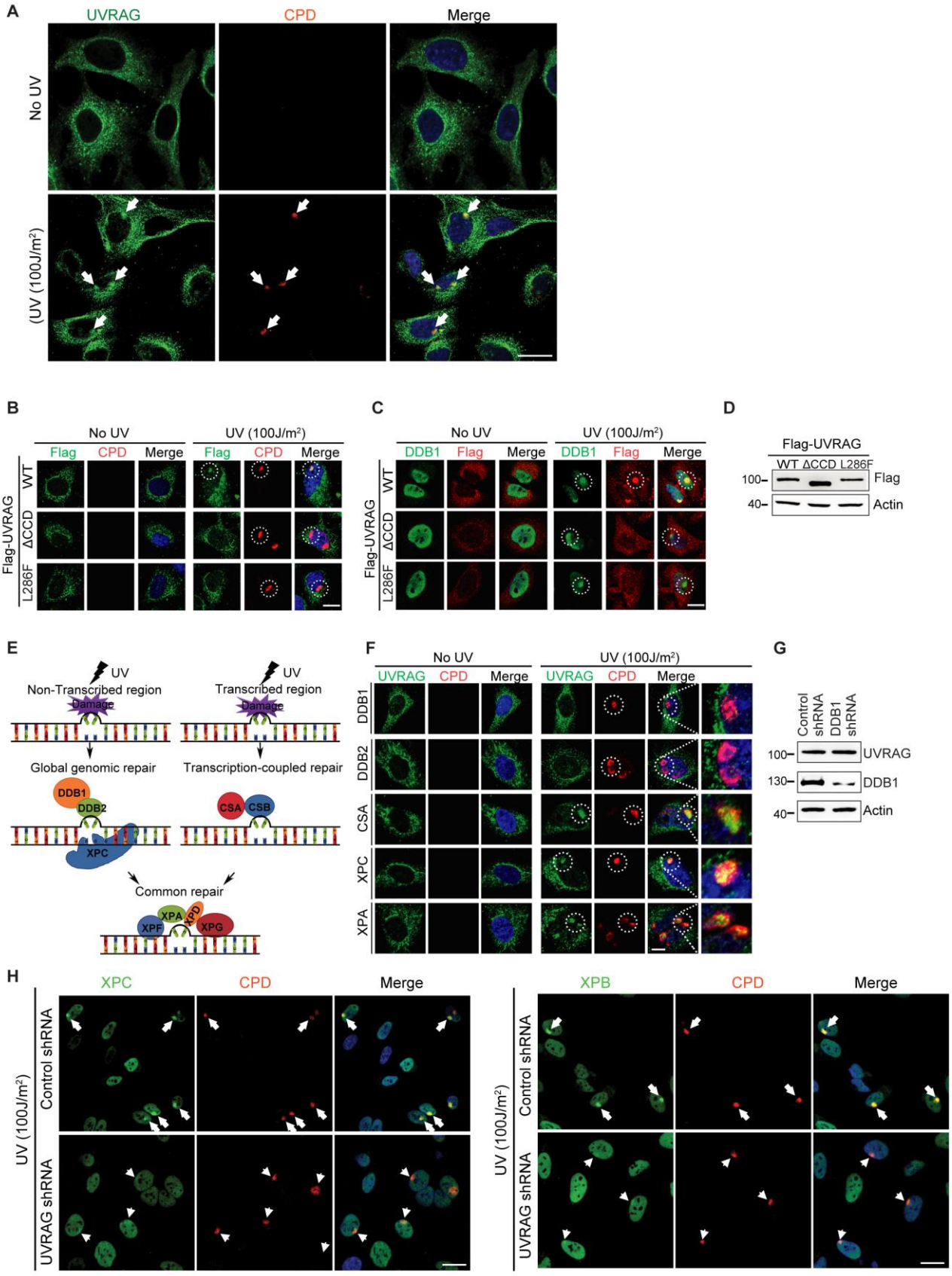
A
UVRAG
CPD
Merge
No UV
(UV (100J/m²)
B
No UV
UV (100J/m²)
Flag
CPD
Merge
Flag-UVRAG
WT
ΔCCD
L286F
C
No UV
UV (100J/m²)
DDB1
Flag
Merge
Flag-UVRAG
WT
ΔCCD
L286F
D
Flag-UVRAG
WT ΔCCD L286F
100–
40–
Flag
Actin
E
UV
Non-Transcribed region
Damage
Global genomic repair
DDB1
DDB2
XPC
UV
Transcribed region
Damage
Transcription-coupled repair
CSA
CSB
Common repair
XPA
XPD
XPF
XPG
F
No UV
UV (100J/m²)
UVRAG
CPD
Merge
DDB1
DDB2
CSA
XPC
XPA
G
Control shRNA
DDB1 shRNA
100–
130–
40–
UVRAG
DDB1
Actin
H
XPC
CPD
Merge
XPB
CPD
Merge
UV (100J/m²)
Control shRNA
UVRAG shRNA

Figure S5

**Figure S5 UVRAG Interaction with DDB1 Is Required for UVRAG recruitment to UV-induced DNA damage sites.** Related to Figure 2

(A**)** Confocal microscopy analysis of the recruitment of endogenous UVRAG (green) to UV-induced CPD damage foci (red). Multi-cell confocal images are shown. Arrows indicate enrichment of UVRAG at CPD foci. Scale bar, 20 μm.

(B**)** Confocal microscopy analysis of the recruitment of wild-type (1st row) and mutant UVRAG (2nd and 3rd row) to CPD damage foci (red) after UV-C irradiation. Scale bar, 20 μm.

(C) Confocal microscopy analysis of the colocalization of the wild-type (1st row) and mutant UVRAG (2nd and 3rd row) with endogenous DDB1 (green) at UV-induced DNA damage sites. Scale bar, 20 μm.

(D) Western blot analysis of WT and mutant UVRAG expression in (B) and in (C). Actin serves as a loading control.

(E) Schematic representation of the sequential recruitment and assembly of the GG-NER and TC-NER factors. In GG-NER, UV-induced DNA damage is recognized by the DDB2/DDB1 heterodimer, which then recruits XPC and downstream effectors for DNA repair. In TC-NER, DNA damage can be recognized by the CSB/CSA complex followed by recruitment of the downstream XPA, XPD, XPF, XPG repair factors.

(F) Recruitment of UVRAG to CPD foci requires functional DDB2 and DDB1 in the GG-NER pathway. Melanoma cells with shRNA-mediated DDB1 knockdown or immortalized DDB2-, XPC-, CSA- or XPA-deficient cells were immunostained for subcellular colocalization of UVRAG (green) with CPD (red) 30 min after micropore UV irradiation. Note the co-staining of UVRAG with CPD in XPC, CSA and XPA cells, but not in DDB1 and DDB2-deficient cells. Scale bar, 10 μm.

(G) Knockdown of DDB1 does not affect the expression levels of UVRAG. WCL of A375 cells stably expressing control shRNA or DDB1-specific shRNA were immunoblotted with anti-UVRAG and anti-DDB1. Actin serves as a loading control.

(H) Knockdown of UVRAG diminished the translocation of XPC (green, left panels) and XPB (green, right panels) to UV-damaged CPD foci. Multi-cell images are shown. Arrows denote clear

colocalization of XPC and XPB with CPD foci in control cells. Arrowheads denote reduced colocalization when UVRAG is depleted. Scale bar, 20 μm.

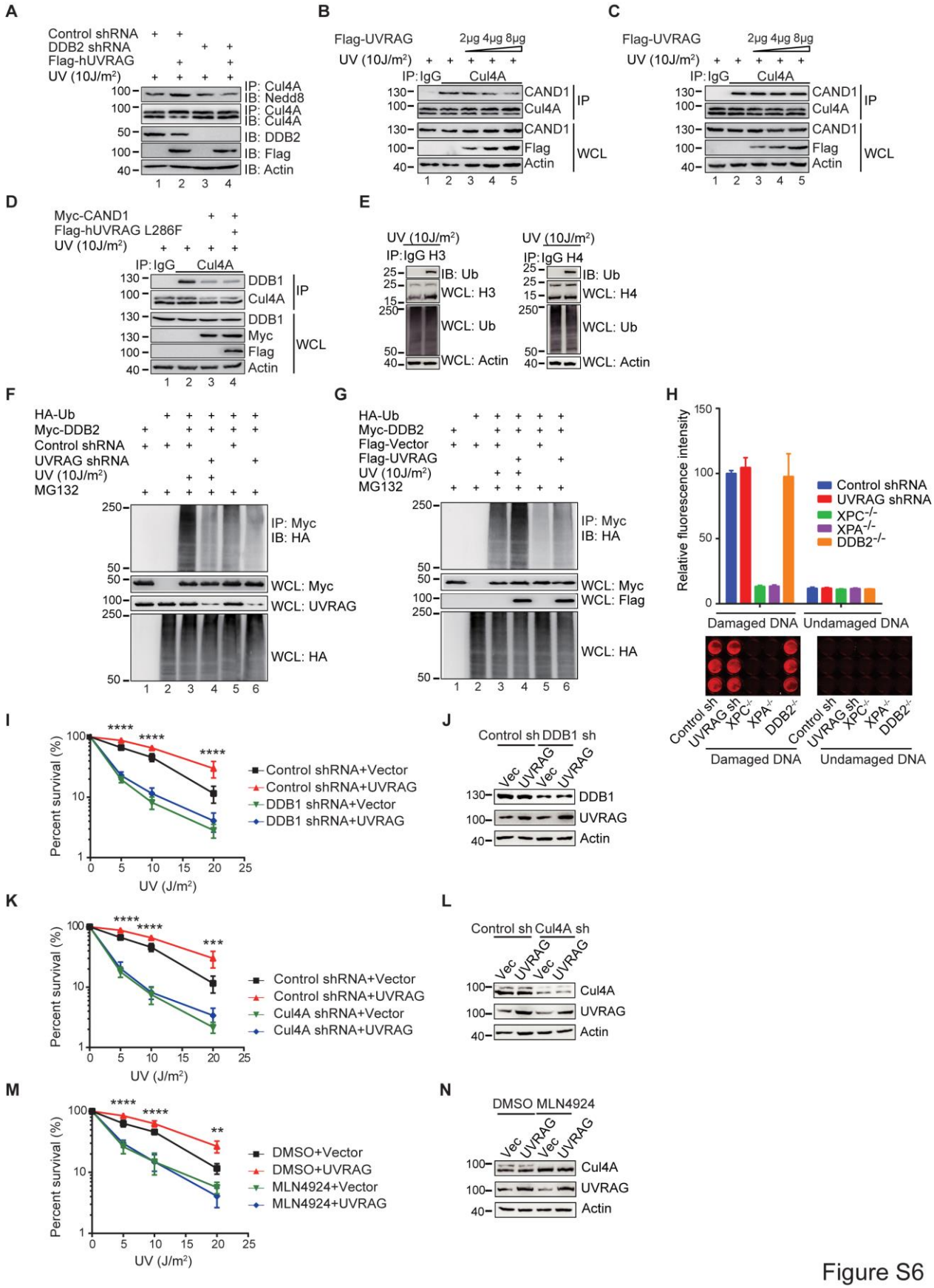
A
Control shRNA
DDB2 shRNA
Flag-hUVRAG
UV (10J/m²)
IP: Cul4A
IB: Nedd8
IP: Cul4A
IB: Cul4A
IB: DDB2
IB: Flag
IB: Actin
B
Flag-UVRAG
2μg 4μg 8μg
UV (10J/m²)
IP: IgG Cul4A
CAND1
Cul4A
IP
CAND1
Flag
Actin
WCL
C
Flag-UVRAG
2μg 4μg 8μg
UV (10J/m²)
IP: IgG Cul4A
CAND1
Cul4A
IP
CAND1
Flag
Actin
WCL
D
Myc-CAND1
Flag-hUVRAG L286F
UV (10J/m²)
IP: IgG Cul4A
DDB1
Cul4A
IP
DDB1
Myc
Flag
Actin
WCL
E
UV (10J/m²)
IP: IgG H3
IB: Ub
WCL: H3
WCL: Ub
WCL: Actin
UV (10J/m²)
IP: IgG H4
IB: Ub
WCL: H4
WCL: Ub
WCL: Actin
F
HA-Ub
Myc-DDB2
Control shRNA
UVRAG shRNA
UV (10J/m²)
MG132
IP: Myc
IB: HA
WCL: Myc
WCL: UVRAG
WCL: HA
G
HA-Ub
Myc-DDB2
Flag-Vector
Flag-UVRAG
UV (10J/m²)
MG132
IP: Myc
IB: HA
WCL: Myc
WCL: Flag
WCL: HA
H
Relative fluorescence intensity
Control shRNA
UVRAG shRNA
XPC-/-
XPA-/-
DDB2-/-
Damaged DNA
Undamaged DNA
Control sh
UVRAG sh
XPC-/-
XPA-/-
DDB2-/-
I
Percent survival (%)
UV (J/m²)
Control shRNA+Vector
Control shRNA+UVRAG
DDB1 shRNA+Vector
DDB1 shRNA+UVRAG
J
Control sh DDB1 sh
Vec
UVRAG
DDB1
UVRAG
Actin
K
Percent survival (%)
UV (J/m²)
Control shRNA+Vector
Control shRNA+UVRAG
Cul4A shRNA+Vector
Cul4A shRNA+UVRAG
L
Control sh Cul4A sh
Vec
UVRAG
Cul4A
UVRAG
Actin
M
Percent survival (%)
UV (J/m²)
DMSO+Vector
DMSO+UVRAG
MLN4924+Vector
MLN4924+UVRAG
N
DMSO MLN4924
Vec
UVRAG
Cul4A
UVRAG
Actin

Figure S6

**Figure S6 UVRAG Antagonizes CAND1 and Activates CRL4$^{DDB2}$ E3 Ligase Activity to Confer UV Protection In a DDB1- and Cul4A-dependent Manner.** Related to Figure 4

(A) Knockdown of DDB2 abrogates UVRAG-promoted Cul4A neddylation upon UV irradiation. 293T cells were transfected with Flag-UVRAG along with control shRNA or DDB2-specific shRNA. At 48 hr post-transfection, cells were UV-irradiated. WCL were subjected to IP with an anti-Cul4A antibody, followed by IB with anti-Nedd8 or anti-Cul4A. WCL were also used for IB with the indicated antibodies to show expression. Note decreased UV-induced Cul4A neddylation upon depletion of DDB2 even in the presence of Flag-UVRAG.

(B, C) Ectopic expression of UVRAG dissociates endogenous CAND1-Cul4A complex. 293T cells transfected with increasing amounts of Flag-UVRAG WT (B) or the L286F mutant (C) were treated with UV. WCL were immunoprecipitated with anti-Cul4A followed by IB with anti-CAND1 or anti-Cul4A antibody. Actin serves as a loading control. Note the reduced binding of CAND1 with Cul4A upon UVRAG expression in a dose-dependent manner.

(D) UVRAG L286F fails to antagonize the inhibitory effect of CAND1 on the DDB1-Cul4A interaction. A375 cells transiently transfected with Flag-UVRAG$^{L286F}$ and/or myc-CAND1 were treated with UV-C irradiation. WCL were immunoprecipitated control or anti-Cul4A antibody followed by IB with anti-DDB1 and Cul4A antibodies.

(E) Ubiquitination of histones H3 and H4 after UV-C irradiation *in vivo*. WCL of A375 cells after UV-irradiation were used for IP with anti-H3 (left) and anti-H4 (right) followed by IB with anti-Ub.

(F) UVRAG deficiency inhibits UV-induced DDB2 ubiquitination *in vivo*. The 293T cells stably expressing control shRNA or UVRAG-specific shRNA were transfected with Myc-DDB2 and HA-ubiquitin (Ub). At 48 hr post-transfection, cells were UV-irradiated and treated with MG132. WCL were used for IP with anti-Myc followed by IB with anti-HA. Note reduced DDB2 ubiquitination upon UVRAG deficiency after UV (lane 4).

(G) Expression of UVRAG promotes UV-induced DDB2 ubiquitination *in vivo*. The 293T cells stably expressing an empty vector or Flag-UVRAG were co-transfected with HA-ubiquitin (Ub), Myc-DDB2

followed by UV-C irradiation and MG132 treatment. WCL were used for IP with anti-Myc followed by IB with anti-HA.

(H) *In vitro* repairing effect of UVRAG knockdown on the naked DNA damage induced by UV. Luminescence assays were used to quantify the levels of *in vitro* NER of UV-irradiated plasmid DNA using cellular extracts isolated from control shRNA- or UVRAG shRNA-treated A375 cells. Cellular extracts of XPC knockout, XPA knockout, and DDB2 knockout cells were included as controls. No luminescence was detected prior to UV irradiation. Note that as does DDB2, UVRAG showed minimal effect on the NER process of UV-damaged plasmid DNA *in vitro*.

(I and J) Colony survival assay of A375_Vector and A375_UVRAG cells expressing control shRNA or DDB1-specific shRNA, after increasing doses of UV-C irradiation (I). Values in the graphs represent mean ± SD from three independent experiments. Note that UVRAG-mediated UV protection was inhibited upon DDB1 deficiency. The expression of DDB1 and UVRAG was assessed by immunoblotting (J). Data are mean ± SD from three independent experiments. ****$p < 0.0001$ (DDB1 shRNA+UVRAG vs. Control shRNA+UVRAG).

(K and L) Colony survival assay of A375_Vector and A375_UVRAG cells expressing control shRNA or Cul4A-specific shRNA, after increasing doses of UV-C irradiation (K). Values in the graphs represent mean ± SD from three independent experiments. Note UVRAG-mediated UV protection was inhibited upon Cul4A deficiency. The expression of Cul4A and UVRAG was assessed by immunoblotting (L). Data are mean ± SD from three independent experiments. ***$p < 0.001$; ****$p < 0.0001$ (Cul4A shRNA+UVRAG vs. Control shRNA+UVRAG).

(M and N) Colony survival assay of A375_Vector and A375_UVRAG cells treated with DMSO or MLN4924 followed by increasing doses of UV-C irradiation (M). Values in the graphs represent mean ± SD from three independent experiments. The expression of Cul4A and UVRAG was assessed by immunoblotting (N). Note UVRAG-mediated UV protection was inhibited upon inhibition of Cul4A neddylation by MLN4924. Data are mean ± SD from three independent experiments. **$p < 0.01$; ****$p < 0.0001$ (MLN4924+UVRAG vs. DMSO+UVRAG).

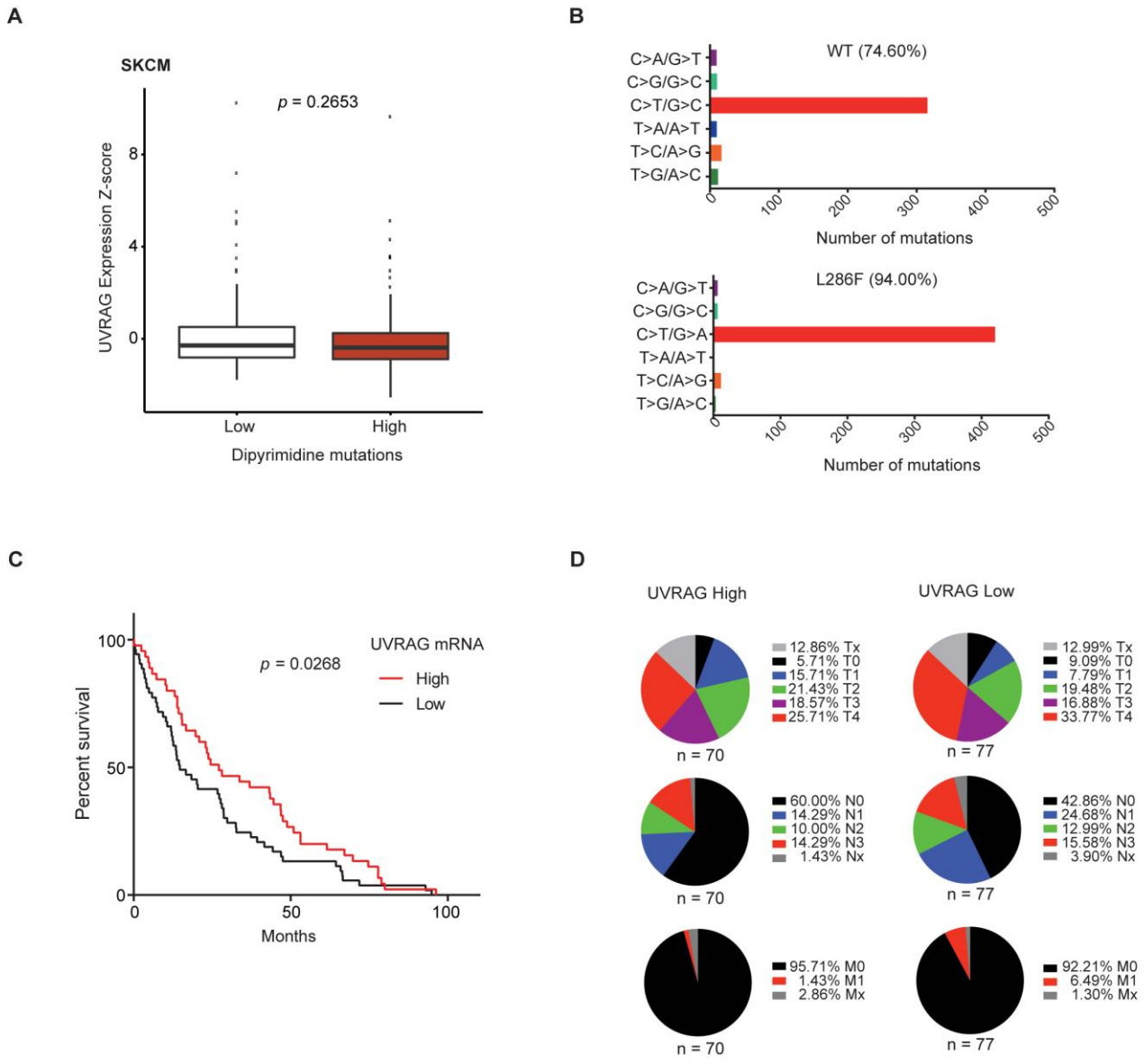


Figure S7

**Figure S7 Impact of UVRAG Expression on the Prognosis and Tumor Stages in Human Skin Melanoma TCGA Cohorts.** Related to Figure 6

(A) UVRAG expression Z-scores in samples with Lower (≤ median of 286 mutations across the genome) or Higher (> median of 286 mutations across the genome) overall mutation rates at dipyrimidine sites for 340 available skin cutaneous melanoma (SKCM) TCGA primary tumors. *p*, two-sided Wilcoxon rank-sum test. Note no significant difference is detected.

(B) UV-specific mutagenesis in UVRAG$^{L286F}$ melanoma. The mutation spectrum of UVRAG$^{WT}$ (top; n = 10) and UVRAG$^{L286F}$ (bottom; n = 1) melanoma in the TCGA cohorts is shown. The melanomas with wild-type UVRAG and Z score closest to 0 were chosen as WT controls. Number of mutations in each of the six possible mutation classes at dipyrimidine sites is counted. Values in parentheses denote percentage of UV-signature mutations.

(C) Overall survival for melanoma patients in the TCGA cohorts based on UVRAG expression. Kaplan-Meier survival curves for melanoma stratified into groups of low (bottom 25%; n= 70) and high (top 25%; n=77) Z-scores of UVRAG. *p*, Gehan-Breslow-Wilcoxon test.

(D) UVRAG expression is associated with advanced TNM stage in the SKCM cohort. TNM, Tumor, Node, Metastasis.

## SUPPLEMENTAL EXPERIMENTAL PROCEDURES

### Cell Culture and Transfection

HeLa, HEK293T, A375, B16, and immortalized MEF (iMEF) cells were cultured in Dulbecco's modified Eagle's medium (DMEM) supplemented with 10% fetal bovine serum (FBS; Invitrogen), 2 mM L-glutamine and 1% penicillin-streptomycin (Gibco-BRL). DDB2 (GM02415), XPC (GM00677), XPA (GM04312; immortalized) and CSA (GM01856) skin fibroblasts were obtained from Coriell Institute (New Jersey, USA) and cultured in Eagles Minimum Essential Medium supplemented with 10% fetal bovine serum, 2 mM L-glutamine and 1% penicillin-streptomycin. The DDB2-, XPC-, and CSA-skin fibroblasts were immortalized by HPV E6/E7. Human dermal fibroblast, adult (HDFa) was purchased from Invitrogen and maintained in Medium 106 supplemented with low serum growth supplement (LSGS) as instructed. Transfections were performed with Calcium Phosphate Transfection Kits (Clontech) or Lipofectamine 2000 (Invitrogen), following the manufacturer's instructions.

### Plasmids

The GST-, Flag- or HA-tagged wild-type (wt) UVRAG and UVRAG$^{C2}$, UVRAG$^{CCD(230-305)}$, UVRAG$^{306-442}$, UVRAG$^{443-583}$, UVRAG$^{584-699}$, UVRAG$^{\Delta C2(42-147)}$ and UVRAG$^{\Delta CCD(230-305)}$, UVRAG$^{\Delta 306-442}$, UVRAG$^{\Delta 443-583}$, and UVRAG$^{\Delta 584-699}$ mutants were constructed by cloning the cDNA of the full-length or truncated mutants into the *Kpn* I/*Not* I sites of the pcDNA5/FRT/TO vector (Invitrogen, USA). pEF/puro-Flag-UVRAG wild-type and mutants were constructed by cloning the cDNA of the WT or truncated UVRAG mutants into the *Afl* II/*Not* I sites of the pEF/puro-Flag vector. The UVRAG mutants R253A, L286F, and shRNA-resistant UVRAG were generated using the Site-Directed Mutagenesis Kit (Clontech) and then cloned in frame with a Flag tag into pcDNA5/FRT/TO or pBabe-neo vectors. The cDNA clones of DDB1 (plasmid# 19918), DDB2 (plasmid# 20700), Cul4A (plasmid# 19951), XPC (plasmid# 39204), CAND1 (plasmid# 19948), and NEDD8 (plasmid# 19943) were obtained from Addgene (USA). The Flag-, Myc- or HA-tagged WT DDB1, DDB2, Cul4A and XPC, and their mutant derivatives were

constructed by cloning the cDNA of the full-length or truncated mutants into the *Kpn* I/*Not* I sites of the pcDNA5/FRT/TO vector. All shRNA plasmids were purchased from Open Biosystem. All constructs were confirmed by sequencing using an ABI PRISM 377 automatic DNA sequencer (Applied Biosystems, Foster City, CA).

**Antibodies, Fluorescent Dyes and Other Reagents**

The following antibodies were used in this study: UVRAG (U7058, Sigma-Aldrich) at 1:1000; UVRAG (SAB4200005, clone UVRAG-11, Sigma-Aldrich) at 1:200; actin (sc-47778, clone C4, Santa Cruz) at 1:10000; CPD (TDM-2, CosmoBio) at 1:1500; Cul4A (ab72548, Abcam) at 1:100; DDB1 (ab109027 Abcam) at 1:100; Roc1 (ab133565, Abcam) at 1:100; DDB2 (ab181136, Abcam) at 1:100; XPC (ab155025, Abcam) at 1:100; XPC (ab6264, Abcam) at 1:100; XPB (ab27317, Abcam) at 1:100; NEDD8 (SAB5300238, Sigma-Aldrich) at 1:1000; Histone H3 (ab1791, Abcam) at 1:1000; Histone H4 (ab10158, Abcam) at 1:1000; CAND1 (8759, Cell Signaling) at 1:1000; Flag (F3165, clone M2; SigmaAldrich) at 1:2,000; Flag (F2555, Sigma-Aldrich) at 1:2,000; GST (SAB4200237, clone 2H3-D10, Sigma-Aldrich) at 1:2,000; GST (26H1, Cell Signaling) at 1:2000; HA (PRB-101P, Covance) at 1:1000, HA (MMS-101P, clone 16B-12, Covance) at 1:2,000; myc (PRB-150P, Covance) at 1:1000; Biotin-Flag (F9291, Sigma); Biotin-IgG (B7264, Sigma); HRP-labelled or fluorescently labelled secondary antibody conjugates, purchased from Molecular Probes (Invitrogen). Purified rabbit IgG was purchased from Pierce. Unless otherwise stated, all chemicals were purchased from Sigma.

**Immunofluorescence and Confocal Laser Scanning Microscopy**

Immunofluorescence microscopy was carried out as described previously (Liang et al., 2008). Briefly, cells plated on coverslips were fixed with 4% paraformaldehyde (20 min at RT). After fixation, cells were permeabilized with 0.2% Triton X-100 for 10 min and blocked with 10% goat serum (Gibco) for 1 hr. Primary antibody staining was carried out using antiserum or purified antibody in 1% goat serum for 1-2 hr at room temperature or overnight at 4°C. Cells were then extensively washed with phosphate-buffered saline (PBS) and incubated with Alexa 488-, and Alexa 568-conjugated

secondary antibodies in 1% goat serum for 1 h, followed by DAPI (4', 6'-diamidino-2-phenylindole) staining. Cells were mounted using Vectashield (Vector Laboratories, Inc.). Confocal images were acquired using a Nikon Eclipse C1 laser-scanning microscope (Nikon, PA) fitted with a 60× Nikon objective (PL APO, 1.4NA) and Nikon image software. All experiments were independently repeated several times.

The Nikon NIS-Elements imaging analysis software was used for the co-localization analyses. In the analysis, confocal images of double-stained sections were first subjected to background correction. Mander's overlap coefficients were calculated and used to obtain the co-localization values as percentages of CPD with the protein of interest (e.g., NER factors). The experimenters were blind to the sample identity during analyses. Values indicate the mean ± SD of at least three independent experiments. All the criteria are well established in our previous study and in the literature. Approximate 50-200 cells from10-20 randomly and blindly chosen high-power fields (60x) were evaluated for imaging analysis. The investigators conducted blind counting for each quantification-related research.

**Immunoprecipitation and Immunoblotting**

For immunoprecipitation, cells were lysed in 2% NP40 or Triton X-100 lysis buffer (25 mM Tris at pH 7.5, 300 mM NaCl, 1 mM EDTA and 2% NP40 or 2% Triton X-100), supplemented with a complete protease inhibitor cocktail (Roche) and Micrococcal Nuclease (NEB M0247), followed by freeze-thaw and sonication (amplitude 15%, process time 10s, push-on time 5s, and push-off time 1s). After pre-clearing with protein A/G agarose beads for 1 h at 4°C, whole-cell lysates (WCL) were used for immunoprecipitation (IP) with the indicated antibodies. Generally, 1-4 μg commercial antibody was added to 1 ml WCL, which was incubated at 4°C for 8-12 hr. After addition of protein A/G agarose beads, incubation was continued for another 2 hr. Immunoprecipitates were extensively washed with NP40 lysis buffer and eluted with SDS–PAGE loading buffer by boiling for 5 min. For immunoblotting, polypeptides were resolved by SDS–PAGE and transferred to a PVDF membrane (BioRad). Membranes were blocked with 5% non-fat milk, and probed with the indicated antibodies. Horseradish

peroxidase (HRP)-conjugated goat secondary antibodies were used (1:5,000, Invitrogen). Immunodetection was achieved with the Hyglo chemiluminescence reagent (Denville Scientific), and detected by a Fuji ECL machine (LAS-3000).

**Clonogenic Cell Survival Assay**

A clonogenic survival assay was performed as described previously (Franken et al., 2006). Briefly, cells were seeded in 60 mm dishes. At 70-80% confluent, cells were treated with UV-C (294 nm) or DNA-damage inducing chemicals (24 hr exposure). Cells were trypsinized, counted, and re-plated in appropriate dilutions for colony formation. After 10 to 14 days of incubation, colonies were fixed and stained in a mixture of 6% glutaraldehyde (Amresco) and 0.5% crystal violet, carefully rinsed with tap water, and dried at room temperature. Plating efficiency (PE) is determined for each individual cell line as described (Franken et al., 2006) and the surviving fraction (SF) is calculated based on the number of colonies that arise after treatment, expressed as PE. Each experiment was repeated three times.

**Local UV Irradiation**

Cells were grown for 24 hr to 70% confluence on glass coverslips and washed twice with PBS. The PBS was then removed, leaving only a thin layer on the top of the coverslip. An isopore polycarbonate filter (Millipore, Bedford, MA) with a pore size of 5 μm diameter was placed on top of the cells. The coverslip with filter was irradiated at a dose rate of $1J/m^2/s$. The filter was then gently removed, and the cells were either processed immediately or cultured for the desired period and processed thereafter.

**In Vitro NER assay**

In vitro NER assay was performed as previous described (Bernard Salles, 1999). Briefly, purified plasmid DNA [using Qiagen column (Cat. No. 27104)] absorbed on the poly-L-lysine-coated 96-well microplates was irradiated by UV-C (254 nm, $300J/m^2$). Per DNA-coated microplate was mixed with 50 μl reaction mixture (5 mg/mL cell extract, 2 mM ATP, 70mM KCl, 44 mM HEPES-KOH, 7 mM

$MgCl_2$, 0.5 mM DTT, 0.5 μM each dGTP, dCTP dATP and biotin-16-dUTP (Enzo, 42811), 10 mM phosphocreatine, 50 μg/mL creatine phosphokinase, 2 mM EGTA, 3.4% glycerol, 0.1 mg/mL BSA, pH 7.8), incubated at 30°C for 3 hr without shaking, and rinse three times with PBST. 50 μL/well of Streptavidin Alexa Fluor® 680 Conjugate (1 μg/mL, Life technologies, S-21378) was then distributed to the plate and incubated for 1 hr at 25°C. The plates were washed five times with PBST and Alexa Fluor® 680 signals were detected using ODYSSEY CLx (Li-cor company).

**Protein Purification**

To identify UVRAG-binding partners, A375 cells expressing Flag only or Flag-UVRAG fusion protein were harvested and lysed with NP40 lysis buffer (50 mM HEPES, pH 7.4, 300 mM NaCl, 1 mM EDTA, 1% (v/v) NP40) supplemented with a complete protease inhibitor cocktail (Roche), followed by sonication. Post-centrifuged supernatants were pre-cleared with protein A/G beads at 4°C for 2 hr. Pre-cleared lysates were then mixed with a 50% slurry of anti-Flag M2-affinity gel (Sigma-Aldrich), and the binding reaction was incubated for 2 hr at 4°C. Precipitates were washed extensively with NP40 lysis buffer. Proteins bound to glutathione beads were eluted and separated on a Nupage 4-12% Bis-Tris gradient gel (Invitrogen). After silver staining (Invitrogen), specific protein bands were excised, digested with trypsin, and analyzed by ion-trap mass spectrometry at the Harvard Taplin Biological Mass Spectrometry facility. Amino acid sequences were determined by tandem mass spectrometry and database searches.

For DDB1 purification, the DDB1 fused to an N-terminal $(His)_{10}$-YFP tag was cloned into an mammalian expression vector derived from the pXLG vector (Backliwal et al., 2008). The resulting plasmid was used to transfect 4.8 liters of HEK293E cells in suspension. After incubation for 3 days, the cells were harvested and disrupted by sonication in a buffer containing 100 mM NaCl, 20 mM Tris-HCl (pH 7.5) and 5 mM β-mercaptoethanol. Cleared cell lysate was loaded onto a Ni-NTA column (Qiagen), and the fusion protein was eluted with the same buffer containing additional 200 mM imidazole. After cleavage of the protein by the PreScission Protease (GE healthcare), DDB1 was

further purified using a Hitrap Q anion exchange column (GE healthcare) and HiLoad 26/60 Superdex 200 gel filtration column (GE Healthcare).

For the purification of Cul4A-Roc1 complex, DNA fragments corresponding to Cul4A and ROC1 were cloned into the pET22b-CPD$(His)_{10}$ and the pET30a (Novagen) vectors, respectively. The two proteins were co-expressed in the BL21(DE3)RIPL strain (Novagen). Cells were harvested and disrupted by sonication in buffer A. The clear lysate was applied onto a gravity flow column containing HisPur$^{TM}$ Cobalt resin (Thermo Scientific). The C-terminal $(His)_{10}$-tagged cysteinyl protease domain (CPD) on Cul4A was cleaved by on-gel digestion using buffer A containing 100 μM inositol hexakisphosphate for 1 hr at 4$^{o}$C. The complex was further purified in the same manner for the DDB1.

**Protein Sequence Analysis by Mass Spectrometry**

Excised gel bands were cut into approximately 1 $mm^3$ pieces. Gel pieces were then subjected to a modified in-gel trypsin digestion procedure (Shevchenko et al., 1996). Gel pieces were washed and dehydrated with acetonitrile for 10 min. followed by removal of acetonitrile. Pieces were then completely dried in a speed-vac. Rehydration of the gel pieces was with 50 mM ammonium bicarbonate solution containing 12.5 ng/μl modified sequencing-grade trypsin (Promega, Madison, WI) at 4ºC. After 45 min., the excess trypsin solution was removed and replaced with 50 mM ammonium bicarbonate solution to just cover the gel pieces. Samples were then placed in a 37ºC room overnight. Peptides were later extracted by removing the ammonium bicarbonate solution, followed by one wash with a solution containing 50% acetonitrile and 1% formic acid. The extracts were then dried in a speed-vac (~1 hr). The samples were then stored at 4ºC until analysis.

On the day of analysis the samples were reconstituted in 5-10 μl of HPLC solvent A (2.5% acetonitrile, 0.1% formic acid). A nano-scale reverse-phase HPLC capillary column was created by packing 5 μm C18 spherical silica beads into a fused silica capillary (125 μm inner diameter x ~20 cm length) with a flame-drawn tip (Peng and Gygi, 2001). After equilibrating the column each sample was loaded via a Famos auto sampler (LC Packings, San Francisco CA) onto the column. A gradient was

formed and peptides were eluted with increasing concentrations of solvent B (97.5% acetonitrile, 0.1% formic acid).

As peptides eluted they were subjected to electrospray ionization and then entered into an LTQ Velos ion-trap mass spectrometer (ThermoFisher, San Jose, CA). Peptides were detected, isolated, and fragmented to produce a tandem mass spectrum of specific fragment ions for each peptide. Peptide sequences (and hence protein identity) were determined by matching protein databases with the acquired fragmentation pattern by the software program, Sequest (ThermoFisher, San Jose, CA) (Eng et al., 1994). Spectral matches were manually examined and multiple identified peptides per protein were required. The data was filter to a 1% peptide false discovery rate.

**Single-molecule Pull-down (SiMPull) Assay**

This assay combines the principles of conventional IP with single-molecule fluorescence microscopy to enable direct visualization of individual cellular protein-protein interactions (Jain et al., 2012). Briefly, flow chambers were prepared on mPEG passivated quartz slides doped with biotin PEG. Biotinylated antibodies were immobilized by incubating 10 nM of antibodies for 10 min on NeutrAvidin (ThermoFisher, San Jose, CA) coated flow chambers. HEK293T cells were lysed and immediately diluted in 20 mM Tris, 50 mM NaCl buffer for 1:200 to obtain well-isolated spots. Treat flow chambers with blocking buffer (ThermoFisher, San Jose, CA) for washing and blocking. Diluted samples were added directly on the chambers and incubated for 15 min. Unbound antibodies and samples were removed by washing with 20 mM Tris, 250mM NaCl buffer for twice. The chambers are visualized using a prism type total internal reflection fluorescence (TIRF) microscope to acquire single-molecule images. Image analysis was performed using scripts written in MatLab.

**Gene Knockdown by shRNA**

All shRNAs were purchased from OpenBiosystem. The sequence targeting human *UVRAG* is: 5'-ACGGAACATTGTTAATAGAA-3'; targeting human *DDB1* is: 5'-GCCTGCATCCTGGAGTATAAA-3'; targeting human *Cul4A* is: 5'-CCAGAATATCTTAACCATGTA-3'; targeting human *Beclin1* is: 5'-

GCCAATAAGATGGGTCTGAAA-3' and 5'-CCGTGGAATGGAATGAGATTA-3'; targeting human *DDB2* is: 5'-CTGAAGTTTAACCCTCTCAA-3'.

**Lentivirus and Retrovirus Production**

For lentivirus production, HEK293T cells were transfected with pLKO.1/puro plasmids together with pCMV-dR8.91 and pCMV-VSV-G packing plasmids using Calcium Phosphate Transfection Kits (Clontech). Viral particles were collected 48 h after transfection, filtered with 0.45 μm sterile filter and concentrated by ultracentrifugation at 4°C (24000 rpm, 2 hr, Beckman-Coulter ultracentrifuge XL-100K). For Retrovirus production, HEK293-Amphotropic cells were transfected with pBabe-neo-Flag-UVRAG and mutants plasmids using Calcium Phosphate Transfection Kits. Viral particles were collected same as for the lentivirus.

**In Vitro Neddylation Assay**

GST-UVRAG and the Cul4A-Roc1 complex were purified from bacteria; DDB1 was purified from HEK293 cell extract following the protocol described above in "protein purification". For the in vitro Cul4A neddylation assay, 10 ng of Cul4A was incubated with 2μg of Nedd8, 10 ng of E1 (APPBP1/UBA3), 200 ng of E2 (Ubc12) (all from Enzo Neddylation Kit BML-UW0590) and 10 ng or 20 ng of GST-UVRAG in a total reaction volume of 20 μl (40 mM Tris-Cl, pH 7.4, 5mM $MgCl_2$, 2 mM ATP, 2mM DTT) at 37°C for 2 hrs. After NEDD8 conjugation, reaction mixtures were added to an equal volume of non-reducing sample buffer and resolved by SDS-PAGE followed by immunoblotting analysis using anti-Cul4A antibody.

***Drosophila* Strains**

The hs-Gal4, GMR-Gal4, UAS-dUVRAG-RNAi and UAS-dDDB1-RNAi lines were obtained from Bloomington stock center. dUVRAG mutants (B7 and B21), FRT40A dUVRAG$^{B21}$/cyo and hsflp/FM6; FRT40A ubi-GFP/bc; UAS-dUVRAG were gifts from Dr. Jongkyeong Chung. To generate mosaic eye

clones, 1st and 2nd instar larvae were heat-shocked for 2 hr. Flies were raised at 25 °C on standard cornmeal/sucrose/yeast/agar media.

**Quantitative RT-PCR Analysis**

mRNA was isolated from the 3rd instar larva's wing discs using the RNeasy mini kit (Qiagen). cDNA was synthesized from mRNA using a mixture of oligo(dT) with the SuperScript II reverse transcription system (Invitrogen). dUVRAG, dDDB1 and GAPDH expression levels were analyzed using qRT-PCR with the SYBR premix Taq polymerase using a Bio-Rad CFX96 device. dUVRAG and dDDB1 expression levels were normalized to GAPDH expression. The primers used were: dUVRAG-forward 5'-GCTACGAACCCTGGCACCTC-3' dUVRAG-reverse 5'-GGTCGATCCATAATGATGGCTAA-3'; dDDB1-forward 5'-CGTTCGCTTGGTTAGCAGTG-3', dDDB1-reverse 5'-GCAGATAATGGATTCCCTCAAA-3'; GAPDH-forward 5'-TGGGATACACCGATGAGG-3', GAPDH-reverse 5'-GCATTTCAGAGCATAGCG-3'.

**Survival Assay In *Drosophila***

The third instar larvae were heat-shocked at 37°C for 2 h to induce dUVRAG, dUVRAG-Ri or dDDB1-Ri expression, followed by exposure to UV at 0-60 J/$m^2$. 1000 larvae were exposed to each dose. After exposure to UV, the larvae were incubated at 25°C until the eclosion of adult flies.

**UV Irradiation of *Drosophila* Eye**

Pupae raised at 25˚C were collected 24 hr after pupa formation. Just prior to irradiation, the anterior pupa case was removed to expose the developing head and retinas. UV irradiation was performed using a 6W 254 nm UVC bulb at a distance of about 70 cm with the exposed retina turned up. After irradiation (50 J/$m^2$), pupae were reared in the dark. Adult eye size was measured using the AmScope software.

**Genomic Analysis of Publically Available Datasets**

All data for DNA sequence alterations, copy number, and gene expression data were obtained from public repositories, e.g., TCGA (https://tcga-data.nci.nih.gov/tcga), CBioPortal (http://www.cbioportal.org/public-portal/) (Cerami et al., 2012; Gao et al., 2013), and COSMIC (http://cancer.sanger.ac.uk/cancergenome/projects/cosmic/). Dipyrimidine *vs.* non-dipyrimidine context was evaluated based on the HiSeq Analysis Software hg19 reference human genome, and all statistical analyses were carried out using the *R* software package and GraphPad Prism 6.0 (GraphPad Software, Inc.).

**Statistical Analysis**

All experiments were independently repeated at least three times. Data are presented as mean ± SD. Statistical significance was calculated using Student's *t* test, and One-way ANOVA, Two-way ANOVA, and Wilconxon rank-sum tests performed using GraphPad Prism 6.0 (GraphPad Software, Inc.), unless otherwise stated. A $p$ value of $\leq 0.05$ was considered statistically significant.

## SUPPLEMENTAL REFERENCES


Backliwal, G., Hildinger, M., Chenuet, S., Wulhfard, S., De Jesus, M., and Wurm, F.M. (2008). Rational vector design and multi-pathway modulation of HEK 293E cells yield recombinant antibody titers exceeding 1 g/l by transient transfection under serum-free conditions. Nucleic acids research *36*, e96.

Bernard Salles, C.P. (1999). In Vitro Chemiluminescence Assay to Measure Excision Repair in Cell Extracts. In DNA Repair Protocols, pp. 393-401.

Cerami, E., Gao, J., Dogrusoz, U., Gross, B.E., Sumer, S.O., Aksoy, B.A., Jacobsen, A., Byrne, C.J., Heuer, M.L., Larsson, E.*, et al.* (2012). The cBio cancer genomics portal: an open platform for exploring multidimensional cancer genomics data. Cancer discovery *2*, 401-404.

Eng, J.K., McCormack, A.L., and Yates, J.R. (1994). An approach to correlate tandem mass spectral data of peptides with amino acid sequences in a protein database. Journal of the American Society for Mass Spectrometry *5*, 976-989.

Franken, N.A., Rodermond, H.M., Stap, J., Haveman, J., and van Bree, C. (2006). Clonogenic assay of cells in vitro. Nature protocols *1*, 2315-2319.

Gao, J., Aksoy, B.A., Dogrusoz, U., Dresdner, G., Gross, B., Sumer, S.O., Sun, Y., Jacobsen, A., Sinha, R., Larsson, E.*, et al.* (2013). Integrative analysis of complex cancer genomics and clinical profiles using the cBioPortal. Science signaling *6*, pl1.

Jain, A., Liu, R., Xiang, Y.K., and Ha, T. (2012). Single-molecule pull-down for studying protein interactions. Nat Protoc *7*, 445-452.

Liang, C., Lee, J.S., Inn, K.S., Gack, M.U., Li, Q., Roberts, E.A., Vergne, I., Deretic, V., Feng, P., Akazawa, C.*, et al.* (2008). Beclin1-binding UVRAG targets the class C Vps complex to coordinate autophagosome maturation and endocytic trafficking. Nat Cell Biol *10*, 776-787.

Peng, J., and Gygi, S.P. (2001). Proteomics: the move to mixtures. J Mass Spectrom *36*, 1083-1091.

Shevchenko, A., Wilm, M., Vorm, O., and Mann, M. (1996). Mass spectrometric sequencing of proteins silver-stained polyacrylamide gels. Anal Chem *68*, 850-858.